M. M. Sarafraz, Mehdi Jafarian, Maziar Arjomandi, Graham J. Nathan
The relative performance of alternative oxygen carriers for liquid chemical looping combustion and gasification
International Journal of Hydrogen Energy, 2017; 42(26):16396-16407

Final publication at http://dx.doi.org/10.1016/j.ijhydene.2017.05.116

The relative performance of alternative oxygen carriers for liquid chemical looping combustion and gasification

M. M. Sarafraz[1, *], Mehdi Jafarian[1], Maziar Arjomandi[1], Graham J. Nathan[1]

[1]Centre for Energy Technology, School of Mechanical Engineering, The University of Adelaide, S.A. 5005, Australia

Abstract

The relative performance of different potential liquid oxygen carriers within a novel system that can be configured for either chemical looping gasification or combustion is assessed in the context of a potential configuration to implement the system, which employs two interconnected bubble column reactors for reduction and oxidation. The parameters considered here are the melting temperature, the Gibbs free energy, reaction enthalpy, exergy and energy flows, syngas quality, and temperature difference between the reactors. Results show that lead, copper and antimony oxides are meritorious candidates for the proposed systems. Antimony oxide was found to offer strong potential for high quality syngas production because of a sufficient oxygen mass ratio for gasification and a sufficiently low operating temperature to the compatible with the requirements for hybridizing with concentrated solar energy. In contrast, copper and lead oxides offer greater potential for liquid chemical looping combustion, because they have higher oxygen mass ratio and a higher operating temperature, which enables better efficiency from a power plant. For all three metal oxides, methane reforming is less than 2%.

Keywords: chemical looping combustion, chemical looping gasification, energetic analysis, thermodynamic equilibrium analysis, syngas production

1. Introduction

Liquid Chemical Looping Gasification (LCLG) and liquid Chemical Looping Combustion (LCLC) are two recently proposed technologies to produce the synthesis gas (syngas) and to provide integrated CO_2 capture from the combustion of a hydrocarbon fuel. Both systems operate based via the indirect transfer of oxygen from the air to the fuel by means of a Liquid Oxygen Carrier (LOC) that is cycled between two reactors, typically termed the air and fuel

reactors. However, the difference between the combustion and gasification configurations of systems is mostly related to the amount of oxygen transferred between the reduction and oxidation reactors by means of the LOC. For any LCLC system, the amount of oxygen transferred is significantly greater than the stoichiometric ratio, while for a LCLG system, it is sub-stoichiometric. Since liquid CLC and CLG are new systems, a wide range of potential LOC materials are available whose potential performance has yet to be assessed. The overall objective of the present investigation is therefore to assess the relative performance of different potential LOCs for this application.

Solid-phase CLG and CLC systems employ solid particles as the oxygen carrier. Although this has the advantage of enabling detailed control of the properties of the OC materials, it also introduces challenges. These include attrition, agglomeration and sintering, particularly at the elevated temperatures, which leads to a short operating life of the particles [1-7]. In addition, the operating temperatures and pressures of these processes are also limited, which results in a decrease in the exergetic efficiency relative to conventional combustion and gasification processes. These limitations have driven the exploration of alternative approaches, such as the use of a liquid OC [8].

Jafarian et al. [8] proposed one approach using a liquid metal oxide as the oxygen carrier to address the aforementioned challenges. They evaluated the thermodynamic potential of the cycle using molten iron oxide as a plausible oxygen carrier. This LOC offers the potential to achieve a high operating temperature of 1350°C, although it suffers the disadvantage of a relatively high solidification temperature. They showed that the proposed system has significant potential to address major limitations of both solid-phase CLC systems and a liquid CLC system proposed by Lamond et al. [9] and McGlashan et al. [10-12], which were temperature limited. Jafarian et al. [8] also showed that it is also possible to configure the liquid chemical looping process to operate in either the CLC or CLG modes by controlling the stoichiometry of the reactor, which can be achieved by varying the relative molar flow rate of the LOC. However, they did not investigate the most suitable type of the liquid oxygen carrier for the liquid CLC and liquid CLG. In addition, the performance of the proposed system was not assessed for different type of LOCs.

Although some studies have been conducted on the influence of the type of solid oxygen carrier particles on the performance of chemical looping combustion working with solid particles [13, 14], to the best of authors' knowledge, no previous assessment has been performed of the

relative performance of alternative LOCs for combustion or gasification. Similarly, no criteria have been proposed with which to perform such a comparative assessment. For this reason, the first aim of this work is to develop a set of thermodynamic criteria with which to assess the relative merit of alternative liquid oxygen carriers for chemical looping. The second objective is to assess the energetic performance of the reactors of these LOCs for CLC and CLG.

2. Methodology

Figure 1 presents a schematic representation of a potential liquid chemical looping combustion or gasification systems. The thermodynamics are analysed for the system proposed by Jafarian et al. [8] whose main components are two interconnected bubble column reactors, referred to as the fuel and air reactors. The former is used to reduce the LOC, which is associated with the oxidation of the fuel and syngas production, while the latter is used to oxidize the LOC using oxygen from the air. During operation, the LOC is circulated continuously between the reactors. The system is analysed using graphite as a surrogate for a range of potential carbon containing feedstock together with steam as the gasifying agent. The assumed product of gasification is syngas, with dominant components of CO and H_2. Figure 1 also represents an ash separator, which is reasonable to assume that it can be developed because of the significant difference in density between the molten metal oxides and fused ash [43, 44]. The process of oxidation causes the reduced and vitiated air (O_2 <21%) to leave the oxidation reactor at an elevated temperature.

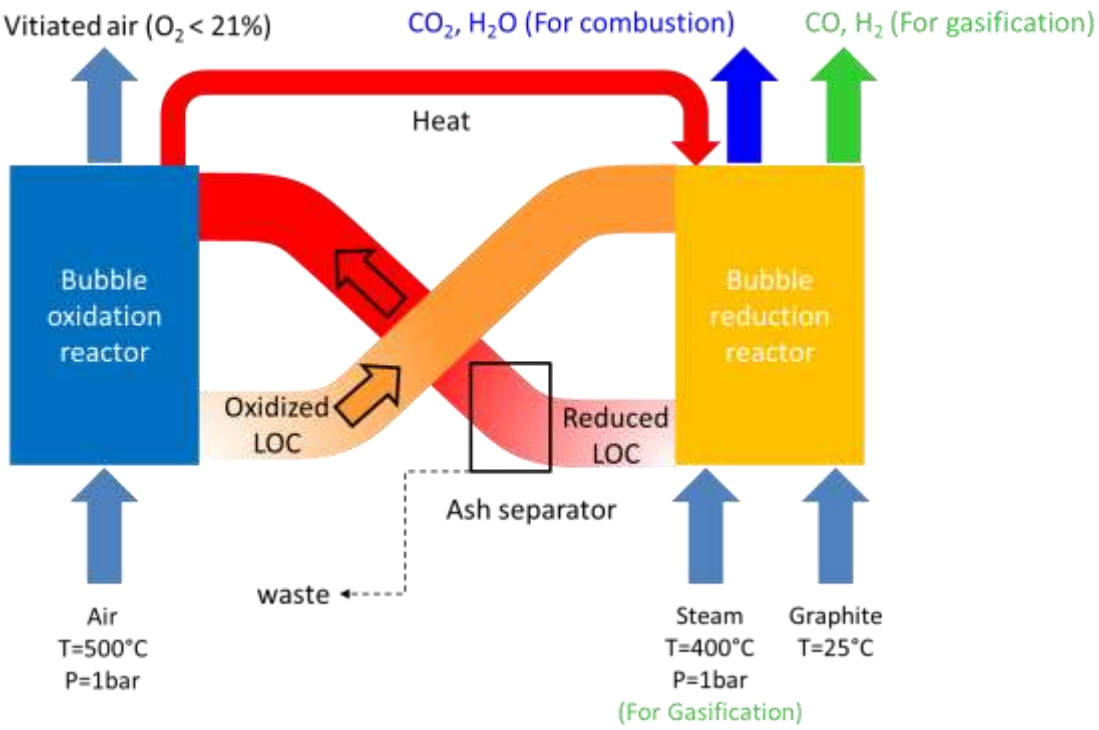

Fig. 1. A schematic diagram of the liquid CLG/ CLC configuration assessed here, for the case of graphite as a surrogate for solid fuels adapted from [8]. The dominant products are CO and H_2, for gasification or CO_2 and H_2O for combustion (colour and size of arrows do not show the temperature, pressure or amount of flow and energy).

For the present analysis, it is assumed that the whole process is ideally isothermal. This assumption is reasonable because the oxidation reaction, which is exothermic, can be used to supply the heat required for gasification, which is endothermic, via circulation of the LOC between the reactors. Furthermore, heat supply and release in each reactor can be controlled by the LOC and partial pressure of oxygen. Isothermal operation also allows solidification to be avoided, which is a necessary element of reliable operation and is desirable to minimise the energy and exergy losses associated with heating and cooling the reactants and products. Setting the circulation ratio between the reactors to be sub-stoichiometric will cause the system to operate in the gasification regime. Setting the circulation ratio to be stoichiometric and above causes it to operate in the combustion regime.

To assess the proposed system thermodynamically, the Gibbs free energy, enthalpy of reaction and oxygen content ratios were estimated using the Gibbs minimization method. The total and partial oxidation of fuel and feedstock ($C_nH_{2m}O_p$) with metal oxides shown as Me_aO_b was calculated as follows:

Combustion mode

In the fuel reactor:

$$C_nH_{2m}O_p(g)+\left[\frac{m+2n-p}{b-ah/g}\right]Me_aO_b(l)\rightarrow\left[\frac{m+2n-p}{b-ah/g}\right]\frac{a}{g}\ Me_gO_h(l)+mH_2O(g)+nCO_2(g), \quad (1)$$

In the air reactor:

$$\left[\frac{m+2n-p}{b-ah/g}\right]Me_gO_h(l)+\frac{1}{2}[m+2n-p]O_2(g)\rightarrow\left[\frac{m+2n-p}{b-ah/g}\right]\frac{a}{g}\ Me_aO_b(l), \quad (2)$$

Gasification mode

In the gasification reactor:

$$\left[\frac{bc-ad}{c}\right]C(s)+Me_aO_b(l)+H_2O(g)\xrightarrow{Heat}\left[\frac{a}{c}\right]Me_cO_d(l)+\left[\frac{bc-ad}{c}\right]CO(g)+H_2(g), \quad (3)$$

In the air reactor:

$$\left[\frac{a}{c}\right]Me_cO_d(l)+\left[\frac{bc-ad}{2c}\right]O_2(g)\rightarrow Me_aO_b(l). \quad (4)$$

The enthalpy of reaction was estimated using equation 5. The oxidation of the reduced liquid metal oxide within the air reactor is always exothermic, while the partial combustion of the fuel inside the fuel reactor can be either endothermic or exothermic, depending on the type of fuel, LOC and the operating temperature of the system. Hence:

$$\Delta M_{red,r}=\sum_{prod}\Delta M_i^f(T)-\sum_{react}\Delta M_i^f(T). \quad (5)$$

In this equation, *M* was assessed for either the Gibbs free energy or enthalpy, $\Delta M_i^f(T)$ is the change of this parameter for component *i* at the temperature *T*. The mole fraction of the components in the product gas were obtained using the following equation [15,16]:

$$\gamma_i=\frac{y_i}{\sum_{j=1}^{n}y_{j,\ products}}. \quad (6)$$

Here, i is a component in the gas product such as CO or CO_2, y_i is the mole fraction of CO or CO_2 depending on whether it is operated in the gasification or combustion mode, respectively.

Eq. (7) was used to assess the ratio of the heat of reaction in the fuel reactor to that transported by the LOC. This parameter is used to assess the condition in which the system can maintain isothermal operation. It determines the amount of LOC required to minimise the temperature difference between reactors which creates the isothermal condition:

$$\Delta T = \frac{\Delta H_{red}}{n_{LOC,oxidised}.\overline{C}p_{,LOC,oxidised}}. \tag{7}$$

Here, ΔT is temperature difference between reactors, ΔH_{red} is the enthalpy of reduction [kJ/mol], which takes place in gasifier (or fuel reactor) for the case of gasification (or combustion), while $C_{p,\,LOC,\,oxidised}$ [kJ/mol. °C] is the average of specific heat for oxidised LOC. Note that the change of $C_{p,\,LOC,\,oxidised}$ with temperature is negligible since process is near isothermal.

Eq. (8) was used to assess the fraction of exergy carried by the syngas for the gasification system:

$$\chi_{syngas} = \frac{\dot{n}_{syngas}.LHV_{syngas}}{\dot{n}_{fuel}.LHV_{fuel}}. \tag{8}$$

Here, χ_{syngas} is the exergy of the syngas, $\dot{n}$ is the molar flow rate of the syngas and LHV is the molar low heating value of the syngas and fuel [kJ/mol]. The exergy balance of the system can be calculated using equation 9 as follows:

$$\chi_{Total} = \dot{n}_{fuel}.LHV_{fuel} = \chi_{syngas} + \chi_{hot\,gas} + \Delta\chi. \tag{9}$$

where, $\Delta\chi$ is the summation of exergy generation and exergy destruction, which is caused by the reactions and losses and is assumed to negligible here, in the absence of detailed system information. The oxygen mass ratio is defined as the ratio of the mass of reduced LOC to oxidised LOC and characterises the capacity of a given metal oxide to transport oxygen in a Red-Ox cycle [8]:

$$OMR = \frac{b \times MW_{oxygen}}{\sum a \times MW_{metal} + b \times MW_{oxygen}}. \tag{10}$$

Here MW_i is the molecular weight of the compound, while a and b are the number of atoms of metal and oxygen, respectively. For the thermodynamic equilibrium analysis, the set of reference conditions shown in Table 1 were defined for the fuel reactor of the liquid CLG and liquid CLC systems. These conditions were chosen based on the stoichiometric value of oxygen in fuel or gasification reactors.

Table 1. Reference conditions for thermodynamic equilibrium analysis of the metal oxides in the fuel reactor.

Operating condition	**Lead oxide**	**Copper oxide**	**Antimony oxide**
Temperature (°C)	900	1350	1000
Pressure (bar)	5	10	5
Gasification			
LOC/feedstock (φ)*	0.2	0.45	0.25
Steam/feedstock (ψ)	1	1	1
Combustion			
LOC/Fuel ratio (φ)**	1	1	1
Steam/Fuel ratio (ψ)	1	1	1

*less than stoichiometric value of oxygen, **4 times higher than stoichiometric value.

To assess the influence of operating parameters, the molar ratios of LOC to fuel (φ) and molar ratio of steam to fuel (ψ) parameters were defined as follows:

$$\varphi = \frac{\dot{n}_{LOC}}{\dot{n}_{Feedstock}} \tag{11}$$

and

$$\psi = \frac{\dot{n}_{Steam}}{\dot{n}_{Feedstock}} \tag{12}$$

where, $\dot{n}$, is the molar flow rate of liquid oxygen carrier.

The Oxygen Mass Ratio (OMR) and melting temperature of the chosen metal oxides were obtained from the experimental data reported in the literature. The criteria that were chosen to select the metal oxides for the present investigation are as follows:

(1) The metal oxide should be in the liquid phase over as wide a range of oxygen content as possible and be operable at, or near to, a constant temperature. This is to minimise exergy loss in cycling between reactors.

(2) The solidification temperature should be as far below the operating temperature as possible, which we have nominally chosen to be at least 100℃ lower, to enable solidification to be avoided without excessive technical difficulty.

(3) The operating temperature should desirably be below 1000℃ to keep the system within the temperature within the range at which metals can be used for containment, although we assess the broader range of 800-1300℃ to maximise relevance to various potential applications of concentrated solar thermal energy.

3. **Results and discussion**

3.1.Melting temperature

Table 2 presents the melting temperature for the 41 metals and metal oxides investigated here. As can be seen, the oxides of copper, antimony, lead and rhodium are potentially suitable for the liquid CLC and liquid CLG systems. For example, copper oxide has three states of oxidation including Cu, CuO and Cu_2O, with similar melting temperatures of 1085℃, 1230℃ and 1325.6℃, respectively. In contrast, chrome does not meet the criteria because its oxides have very different melting temperature i.e. 197-2435℃. In addition, it is possible that a solid-phase oxidation state of chrome will form, since Cr_2O_3 has a much higher melting temperature (2435℃) than the target operating temperature of ~1300℃. This risks significant operational challenges, such as blockages and degraded performance. From this, eleven metals were selected for further investigation.

Table 2. Melting point of the metal and metal oxides considered in this study.

Materials	Melting point (°C)	Reference
Co	1495	[17]
CoO	1933	[18]
Co_3O_4	895	[19]
Cu	1085	[20, 21]
Cu_2O	1230	[20, 21]
CuO	1325.6	[22]
Cd	321.3	[23]
CdO	1559	[23]
Fe	1539	[24, 25]
Fe_2O_3	1566	[25]
Fe_3O_4	1597	[24]
FeO	1377	[18]
Ni	1455	[26]
NiO	1955	[26]
Mn	1246	[27]
MnO	1945	[27]
MnO_2	535	[27]
Mn_2O_3	940	[27]
Sb	630.6	
Sb_2O_3	656	[27]
Sb_2O_4	540	[27]
Sb_2O_5	380	[27]
Pb	327.5	
PbO	888	[27]
Pb_3O_4	500	[27]
PbO_2	290	[27]
Sn	231.9	
SnO	1080	[27]
SnO_2	1630	[27]
V	1910	
VO	1789	[27]
V_2O_3	1940	[27]
VO_2	1967	[27]
V_2O_5	690	[27]
Cr	1907	
CrO_3	197	[27]
Cr_2O_3	2435	[27]
CrO	300	[27]
Rh	1963	
Rh_2O_3	1100	[27]
RhO_2	1050	[27]

Figure 2 presents schematically the distribution of melting temperature and OMR for the oxides of eleven metals. As can be seen, the oxides of Cr, Mn, V, Ag, Fe and Cd do not meet the first and third criteria, because the difference between melting temperatures of their oxidation states is too great as noted above. These metals are therefore eliminated from the selection process. However, Cu, Pb, Rh and Sb oxides do satisfy the aforementioned criteria. All oxidation states of Pb have melting temperature lower than 900°C, while for copper oxide, it ranges between 1085°C and 1300°C. Similarly, for Sb the melting temperature of the oxide is in range 380°C-

650°C, while for rhodium oxide, the range is 1050°C-1100°C. Therefore, these four metal oxides were selected for further assessments.

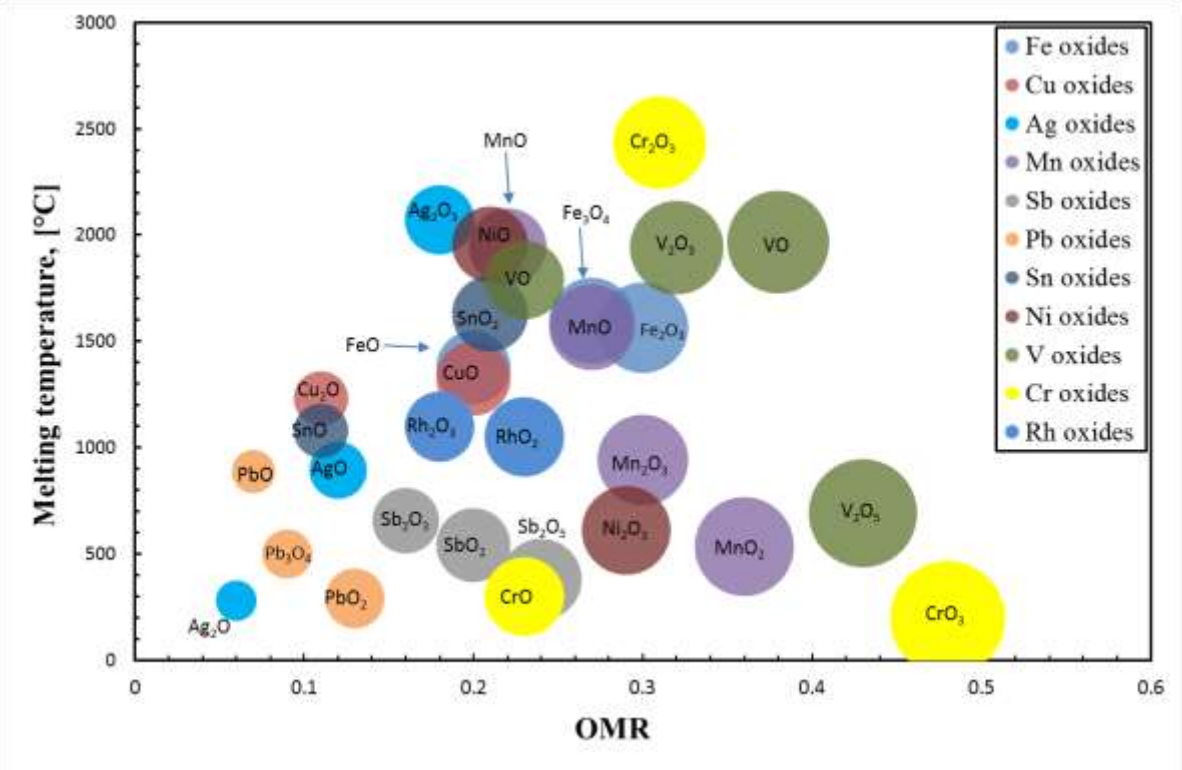

Fig. 2. Comparison of the melting temperature of the oxygen mass ratio of the oxidative states of eleven metal oxides. Each sphere is centred on the data point, while its area is proportional to oxygen mass ratio.

3.2.Gibbs free energy

Figure 3 (a and b) presents the dependence on temperature of the Gibbs free energy of the oxidation and reduction reactions for different metal oxides (Sb, Pb, Cu, and Rh) reduced with pure graphite, as derived with Eq. s (1-4). It can be seen that the Gibbs free energy for the reduction and oxidation of antimony with graphite and air, respectively is negative. In addition, it has a negative slope, so that it becomes increasingly negative with an increase in the operating temperature. This implies that the reaction is spontaneous. Its oxidation reaction also has negative values, although its slope is positive. For both lead and copper oxides, the Gibbs free energy is also negative for the reduction with graphite and oxidation with air, although the oxidation has a positive slope with temperature. However, for rhodium oxide, the Gibbs free energy is positive, meaning that this reaction is not likely to occur at temperatures within the range 1100°C-1500°C. Therefore, rhodium is unsuitable for the liquid CLG and liquid CLC

systems. In addition, rhodium is radioactive and scarce element and both are further disadvantages. However, both lead and antimony oxides exhibit favourable Gibbs free energy in the liquid phase, although over different ranges of operating temperature. Antimony oxide stays in the liquid phase over the temperature range of 600°C < T < 1500°C, while copper oxide has a smaller range of 1100°C < T < 1500°C and lead ranges from 900°C to 1500°C. It is readily apparent that a wider range of operating temperature offers greater flexibility. In addition, as is shown below, the production of CO_2 is also temperature-dependent and is reduced by an increase in the operating temperature (see section 3.5).

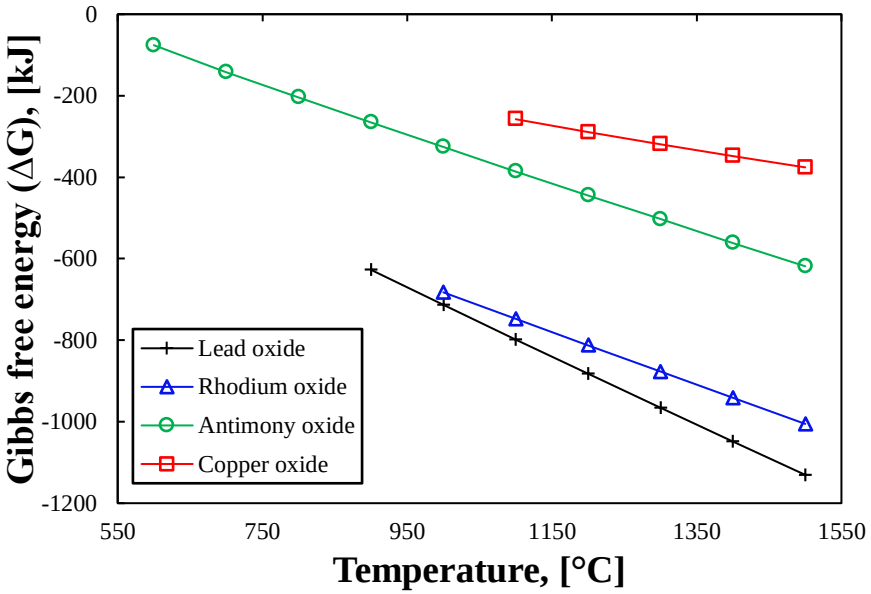

(a)

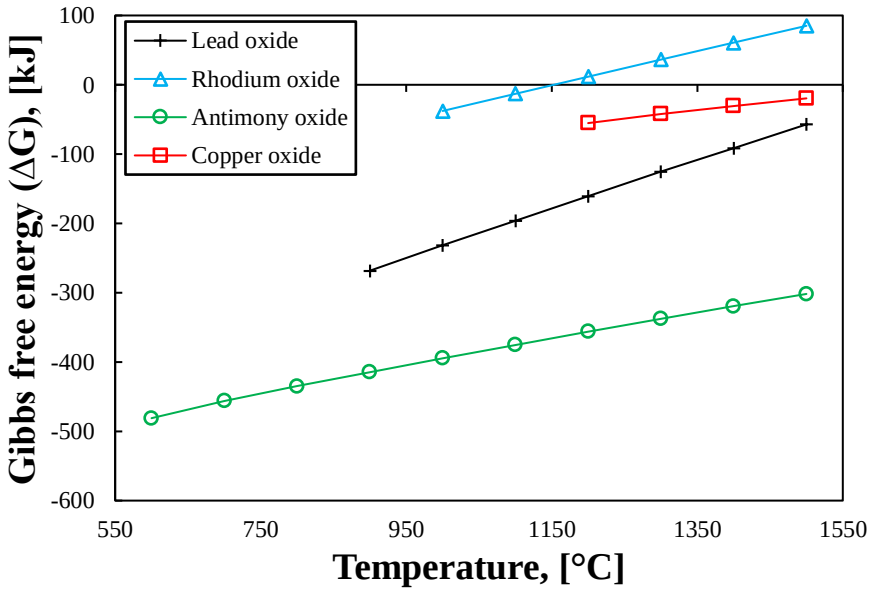

(b)

Fig. 3. Dependence on temperature of the Gibbs free energy of the reduction and oxidation reactions for three metal oxides. a) Reduction reaction, b) Oxidation reaction.

3.3.Enthalpy of reactions:

Figure 4 (a-c) presents the calculated dependence on temperature of the enthalpy of reduction and oxidation for the metal oxides Pb, Cu and Sb in both the gasification and combustion regimes assuming that the reactions proceed to equilibrium. It can be seen that all metals exhibit the same general trend in which the enthalpy of reduction is positive and decreases with temperature, while the enthalpy of oxidation is negative and increases with temperature. The net enthalpy of reaction is greatest for antimony, slightly less for lead and significantly less for copper. In contrast, for the oxidation reaction, the reaction enthalpy of lead is slightly greater than antimony, whilst for copper it is again the least. Of the three metals, copper exhibits the most non-linear dependence on temperature, which occurs over the range 1100°C-1300°C. This change in the slope is due to the chemical conversion of CuO to Cu_2O. Where the enthalpy of reaction is sufficiently negative to overcome heat losses from the reactor, there is no risk of solidification of liquid LOC. On the other hand, where the enthalpy is positive, there is potential to employ concentrated solar thermal energy to supply the required heat. However, the detailed assessment of these options is beyond the scope of the present investigation.

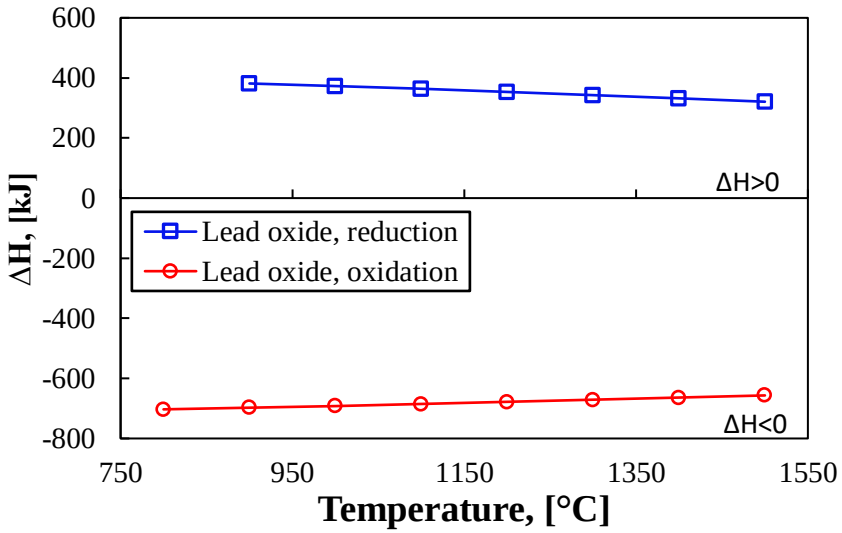

(a)

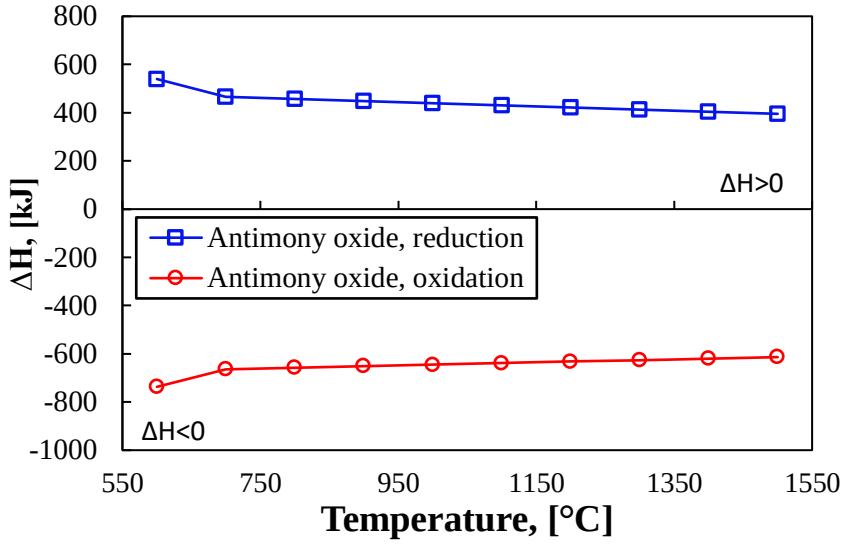

(b)

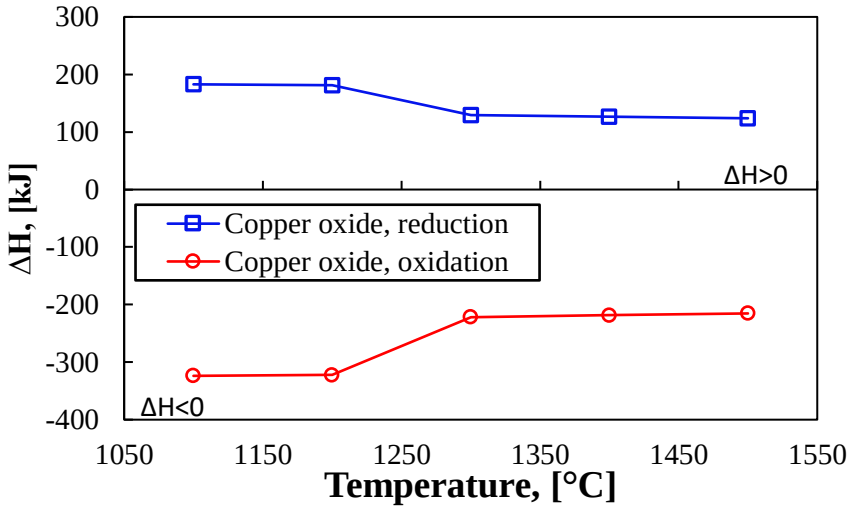

(c)

Fig. 4. Dependence of the enthalpy of the reduction and oxidation reactions on temperature for a) lead oxide b) antimony oxide c) copper oxide.

3.4.Energetic analysis of reactors

Figure 5 presents the calculated dependence on temperature of the ratio of the enthalpy of oxidation with air to that of reduction ($\frac{\Delta H_{ox}}{\Delta H_{red}}$) for the case of graphite. As can be seen, $\frac{\Delta H_{ox}}{\Delta H_{red}}$ > 1 for all three metal oxides, showing that the overall process is exothermic and can be self-sustaining. However, the ratio is greatest for lead oxide, to reach a value as high as 1.85 at 1000°C. The ratio for copper is slightly lower at 1.7 for 1300°C and lowest for antimony (1.48 at 1000°C).

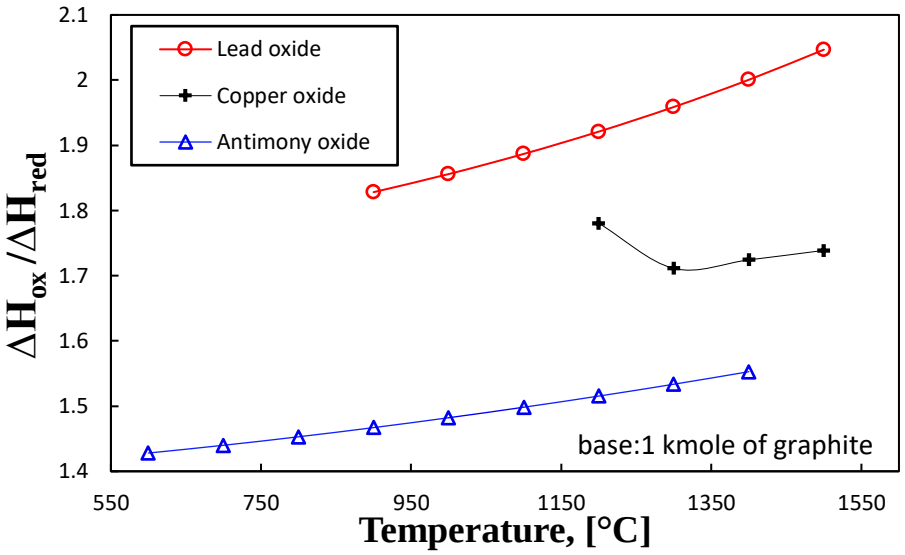

Fig. 5. Dependence on temperature of the calculated $\frac{\Delta H_{ox}}{\Delta H_{red}}$ for three liquid metal oxides.

Figure 6 presents the dependence of ΔT on the φ for copper, lead and antimony oxides. As can be seen, for lead oxide, the minimum LOC required for a 10°C temperature difference between reactors is 168 moles of LOC per moles of feedstock, while for copper and antimony oxides, it is 193 and 268 moles of LOC per moles of feedstock, respectively. For a 50°C temperature difference between the reactors, the required LOC/feedstock ratio is 35, 38 and 52, respectively and for 100°C temperature difference, the required LOC is 17, 19 and 26 moles, respectively. Based on this criterion, antimony oxide provides a lower temperature difference for higher LOC/fuel ratios, meaning that this oxide can provide sufficient oxygen for total combustion as well. Nevertheless, given that the stoichiometric ratio of graphite to air is 4.5 to 6.1 times greater than that of air.

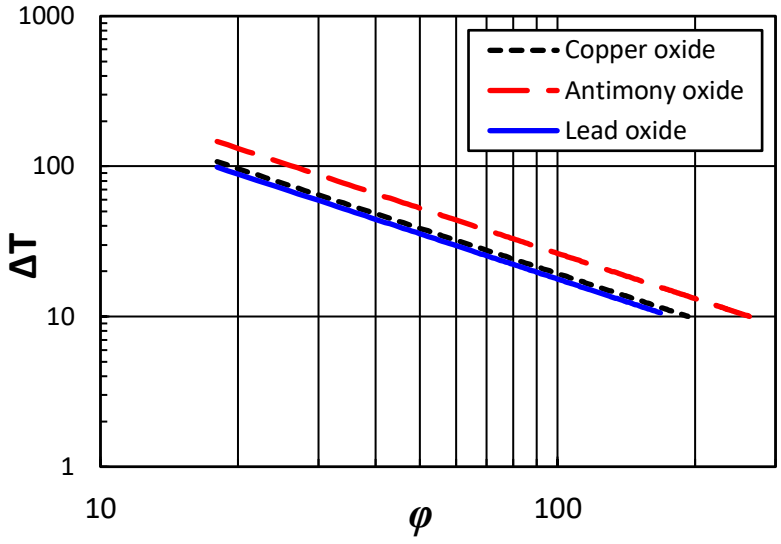

Fig. 6. Dependence of temperature difference (ΔT) between reactors on liquid oxygen carrier to fuel ratio (φ) for different metal oxides at reference conditions given in Table 1.

3.5. Mole fractions of syngas and hot gas

Figure 7 (a-b) presents the calculated dependence on reactor temperature of the calculated mole fractions of CO and CO_2 in the product gases from the liquid CLG system for lead, copper and antimony oxides as the LOC. As can be seen, for all three metal oxides, the mole fraction of CO in the outlet stream of the fuel reactor increases with an increase in temperature, while that of CO_2 decreases. The trend is clearest for antimony oxide, for which it can be seen that the mole fraction of CO increases asymptotically with the temperature and approaches a constant value at a sufficiently high operating temperature, although the asymptotic value is not quite reached over this temperature range (see Fig. 7a). The data for copper oxide is similar to that for antimony oxide, but is only possible for a narrower range of operating temperature. However, it is significantly lower for lead oxide. The inverse results can be seen for CO_2 (Fig.7b), in that a relatively high production of CO is associated with a relatively low production of CO_2. For gasification, it is desirable to maximise the production of CO and minimize that of CO_2. In addition, it is also desirable to operate at as low a temperature as possible. Hence, on this basis, antimony oxide is the preferred LOC since it results in a mole fraction of CO of 0.45, and also allows operation at temperatures below 1000°C with very little trade off in performance. On the other hand, while copper has only slightly poorer performance in terms of product gas composition, it requires operation at temperatures of at least 1200°C to retain some buffer, which constitutes a significant disadvantage. Also poor is the performance of lead oxide. While it exhibits a temperature range that is almost as wide as antimony, it yields

a significantly lower production of CO and higher production of CO_2. More specifically, antimony generates the lowest amount of CO_2 at the reference operating conditions with a mole fraction of 0.04, followed by copper and lead oxides, for which it is 0.06 and 0.11, respectively (See Fig. 7b).

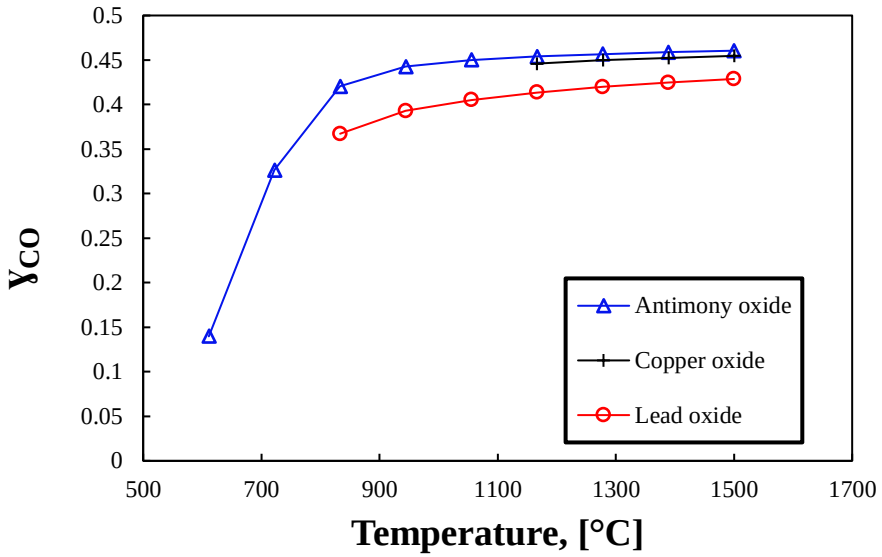

(a)

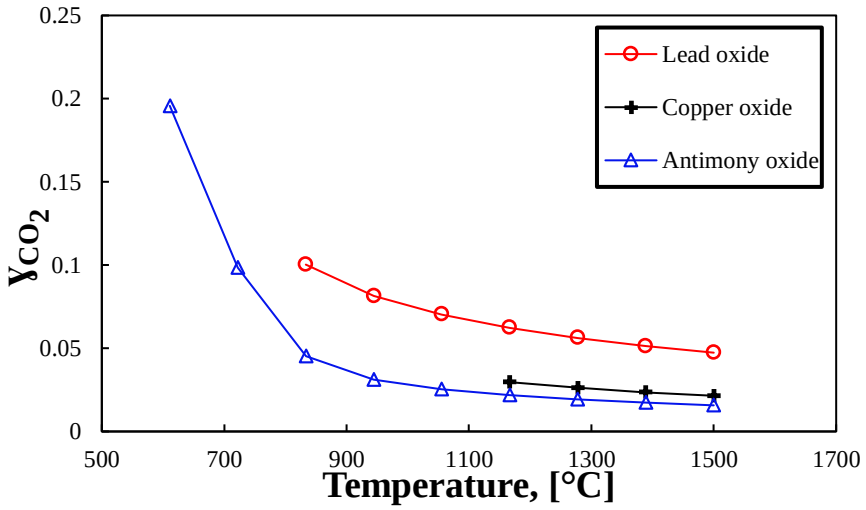

(b)

Fig. 7. Dependence of the fractions of CO and CO_2 in the product gas on the temperature of the reduction reactor for three metal oxides reduced by graphite in a liquid CLG system, a) CO mole fraction, b) CO_2 mole fraction

Figure 8 (a-b) presents the dependence on temperature of the calculated mole fractions of CO and CO_2 for the same three metal oxides in a liquid CLC system. Unlike liquid CLG, the mole fraction of CO_2 is at least an order of magnitude higher than that of CO. Although the conversion to CO_2 decreases with an increase in temperature for antimony and copper oxides, complete conversion is achieved independent of temperature for lead oxide. This shows that, for temperatures greater than 850°C, lead is preferable over the other two metal oxides at higher temperatures from the point of view of complete combustion. Importantly, while antimony approaches the complete combustion for temperatures ~600°C, the lowest value achieved for concentration of CO is 2000 ppm at 1300°C, so that further treatment may be necessary, which would add to cost. Moreover, temperature has direct influence on proceeding of reduction reaction, while quantity of oxygen released by lead oxide is limited and as the result, increasing the temperature has no effect on the mole fraction of CO and CO_2. Therefore, lead oxide is the preferred LOC and can be used for temperature range 900°C-1500°C.

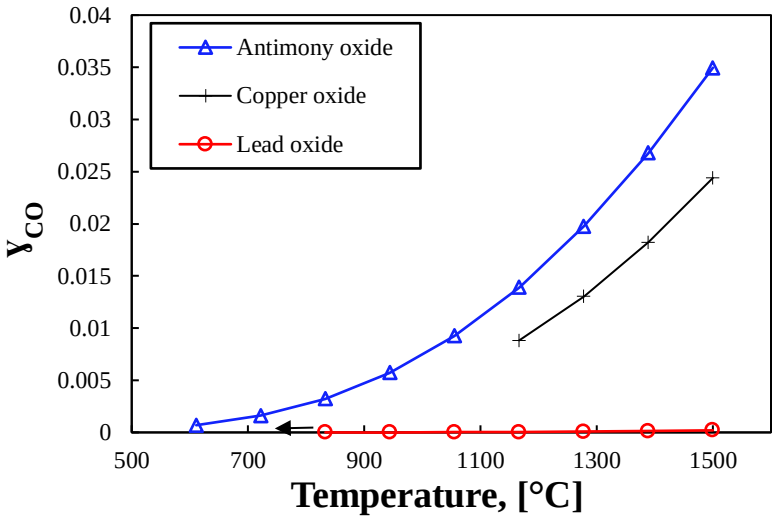

(a)

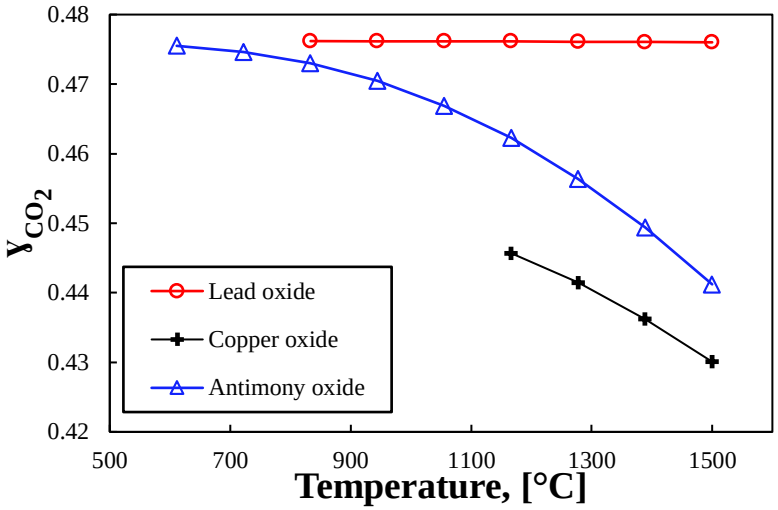

(b)

Fig. 8. Dependence on temperature of the mole fractions in the product gas for three metal oxides reduced by graphite in a liquid CLC system of a) CO, b) CO_2.

3.6.Syngas quality

Figure 9 presents the dependence of syngas quality on temperature for the liquid CLG system with three different metal oxides. As can be seen, the ratio of H_2/CO, is referred to as syngas quality, decreases with an increase in temperature [28]. Significantly, this decrease is non-linear for antimony oxide, and is nearly linear within the range of temperatures for copper and lead oxides. For antimony oxide, the trend can be divided into two regimes. In regime I, rate of decrease for syngas quality is considerably higher than regime II. This is because at temperature lower than 900°C, the Boudouard reaction proceeds and more CO is produced, while at temperatures higher than 900°C, Boudouard reaction is suppressed. As a result, CO production is suppressed in this regime, which reduces the syngas quality. Significantly, at the reference operating condition, antimony oxide provides the highest syngas quality of the three metals. In addition, it is the only metal oxide that enables the target of 2.1 for the Fischer-Tropsch process to be reached, with both lead and copper oxides both operating in regime 2 throughout the temperature range. Importantly, operation at low temperatures cause the production of both methane and tar for conventional gasification. However, for gasification via liquid antimony oxide, system works at temperatures around 800-1000°C without methane reforming.

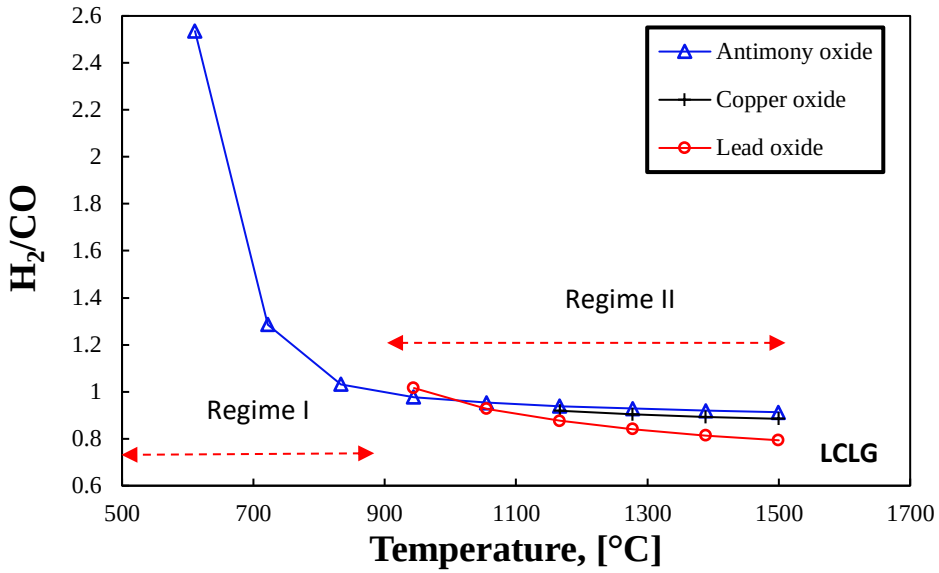

Fig. 9. Dependence of syngas quality (H_2:CO) on temperature for different metal oxides in LCLG concept at reference condition given in Table 1. In regime 1, system operates as CLG which produced a very high quality syngas. In regime 2, system works as mixed combustion, while in regime 3, complete combustion of fuel occurs. The quality of syngas in regime 1 is highest and antimony is the only metal oxide that can work at this temperature range.

Figure 10 presents the dependence of syngas quality on φ for three metal oxides at the reference conditions. As can be seen, for the case where $\varphi < 1$ *(regime I)*, the quality of the syngas product is higher than regime 2, for which $\varphi > 1$. In regime I, due to the gasification process, a mixture of CO and H_2 with an insignificant amount of CO_2 is produced (for all metal oxides ranged from 0.2% to 8% depending on the φ). For example, for φ =0.05, the value of H_2/CO=1.09 (with 0.02 CO_2) for antimony oxide, while it is 1.07 (with 0.06 CO_2) and 1.04 (with 0.05 CO_2) for copper and lead oxides, respectively. Likewise, with an increase in φ, the syngas quality decreases and similar trends can be seen for all three metal oxides. However, for $\varphi > 2$, mode of system changes to mixed combustion and as a result, more carbon dioxide is produced, which decreases the syngas quality.

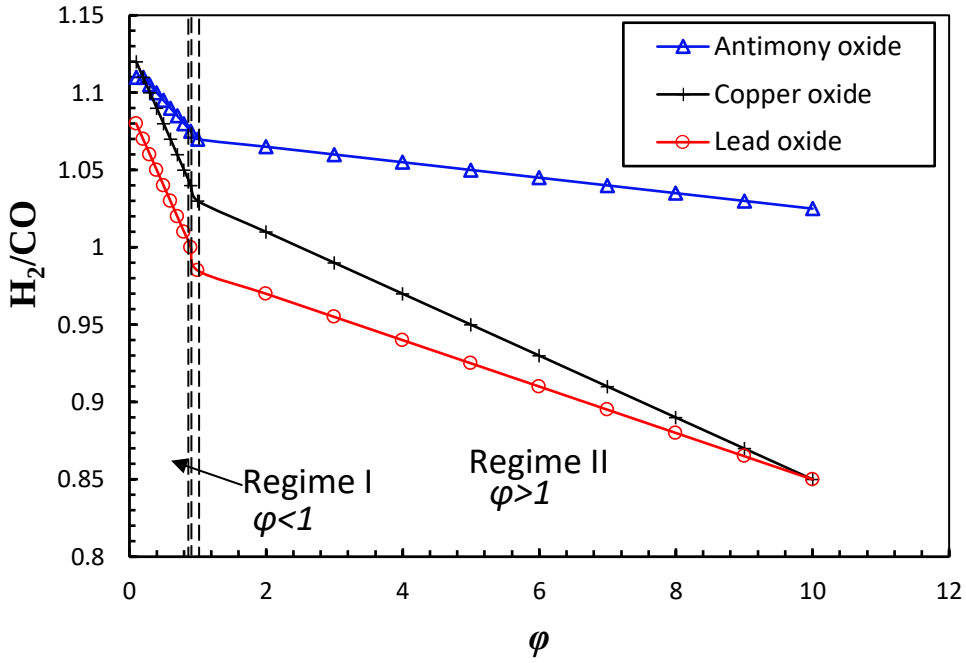

Fig. 10. Dependence of syngas quality (H_2/CO) on the ratio of liquid oxygen carrier to fuel (φ) for three metal oxides for steam/fuel ratio, ψ of unity. All other conditions are as per table 1.

Figure 11 presents the dependence of syngas quality on ψ for the three metal oxides at the reference conditions. Also shown is the target syngas quality of 2 that is suitable for Fischer-Trospsch synthesis, and for alcohol production process. As can be seen, antimony oxide requires less steam than does copper and lead oxide. For example, with 1 kmol of feedstock is introduced to the gasifier, 2.6 kmol of steam is required for antimony oxide to achieve H_2 / CO=2, while the equivalent ratio is 3.2 and 4 for copper and lead oxide, respectively. It can also be seen that there is an optimal value of ψ, however, the peak value of ψ is also greatest for antimony than for the other metals. That is, antimony oxide offers the highest syngas quality, followed by copper and lead oxides at the similar operating conditions.

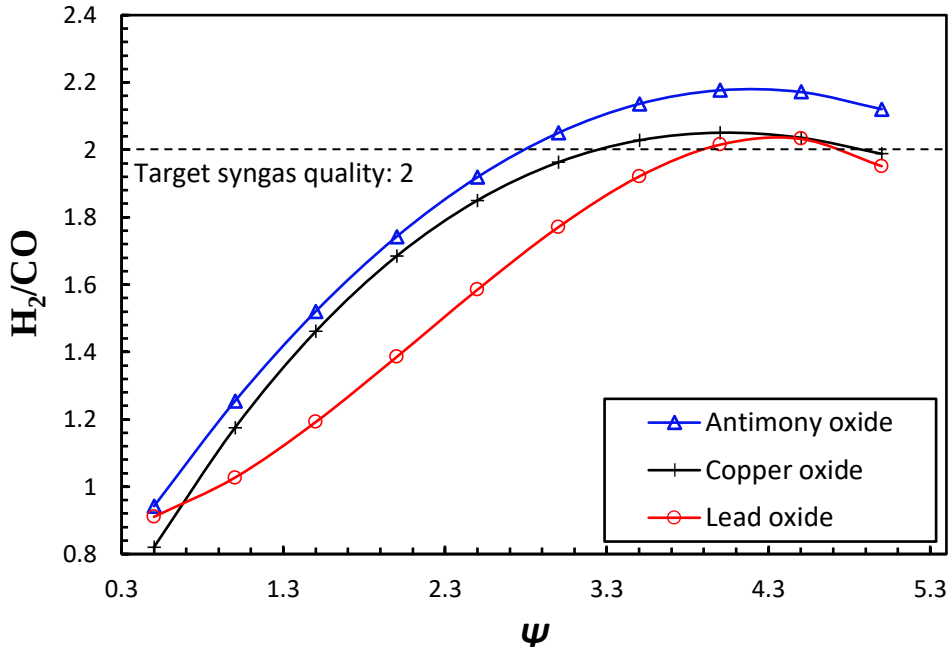

Fig. 11. Dependence of syngas quality (H_2/CO) on the molar ratio of steam to fuel (ψ) for three metal oxides at the reference conditions.

3.7.Exergy analysis for gasification using liquid metal oxides

Figure 12 presents the dependence on temperature of the exergy efficiency of syngas production for the three metal oxides, each calculated with equation 8 for the values of φ and ψ corresponding to a value of H_2/CO=1. As can be seen, gasification with antimony oxide produces the high quality syngas with slightly higher exergy efficiency than copper oxide. However, for lead oxide, gasification can be done at lower temperatures, which increases the possibility of side production of methane and tar (900°C versus 1300°C). For antimony oxide, approximately, 67% of exergy is in syngas, while for copper oxide; about 60% of exergy is in syngas (LHV based). However, for lead oxide, almost half of the exergy is in syngas (48.8%) and the rest is in exhausted gas and outlet air. For the system working with lead oxide, some of the exergy from the air reactor could potentially be recovered (e.g. by preheating reactants or by use of a power plant), but this is beyond the scope of the present investigation.

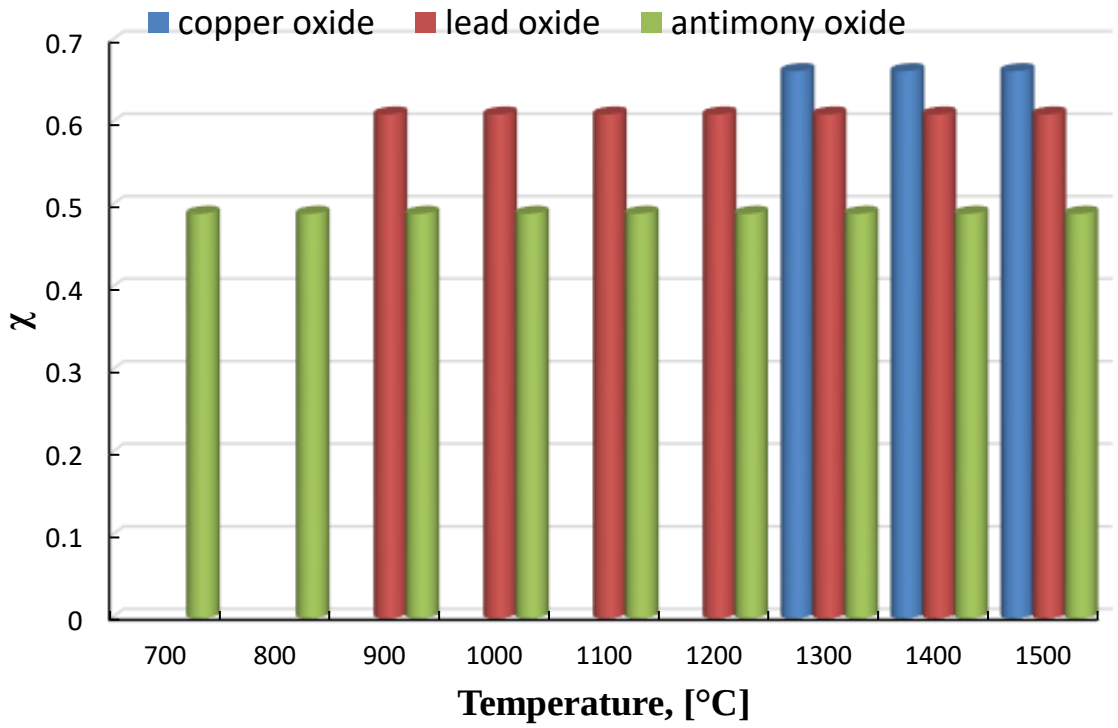

Fig. 12. Dependence of the exergy efficiency (χ) on temperature for the production of syngas from the gasification of graphite for three metal oxides for the reference conditions given in Table 1 and for $H_2/CO=1$.

3.8.Methane reforming

Figure 13 presents the dependence of mole fraction of CH_4 on temperature for the gasification with three molten metals at the reference condition given in Table 1. As can be seen, for all three molten metals, CH_4 reforming is less than 2%, meaning that gasification with molten metals can be done without methane reforming. For example, lead and copper oxides, both have the least methane reforming, while for antimony oxide at 600-700°C, mole fraction of methane in product is about 2%. However, with an increase in temperature, methane mole fraction decreases for all the molten metals. For copper and antimony oxides, at 1500°C, the mole fraction of methane is approximately zero, while for lead oxide, this happens at 900°C. Overall, the LCLG concept has a great potential to eliminate the methane reforming or at least limit the mole fraction of CH4 to plausible mole fraction of 1%.

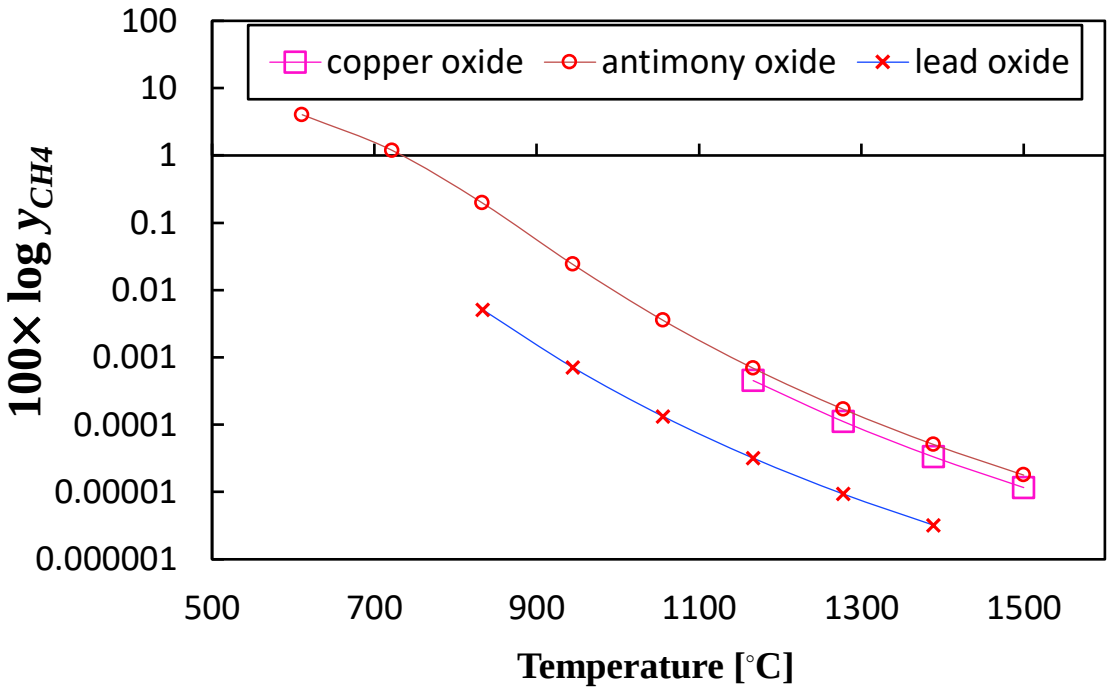

Fig. 13. Dependence of the mole fraction of methane on temperature in gasification with three different molten metals.

4. Conclusions

A comparative study of the relative performance of 41 oxides of 11 metals as oxygen carriers for liquid chemical looping gasification or combustion has revealed the following conclusions:

- The critical value of the molar ratio of the liquid oxygen carrier to the fuel has been identified, below which the system operates in the gasification regime and above which it operates in the combustion mode. This critical value is 0.18, 0.24 and 0.08 as the LOCs, respectively.
- The LOC with the greatest overall thermodynamic potential for operation in the gasification regime was found to be antimony oxide. This was calculated to yield the highest quality of syngas (up to 2.12) of the metals assessed here and requires the lowest flow rate of steam for gasification. In addition, it offers potential to operate at temperatures as low as 600°C, which is the lowest of these metal oxides.
- The LOC with the greatest overall thermodynamic potential for operation in the combustion regime was found to be lead oxide. This was found to enable the most complete combustion, which is also independent from the operating temperatures greater than 900°C to prevent solidification.

- Gasification with all molten metals studied in this work showed that metal oxides oxide at the highest temperature minimize the methane reforming. Antimony and lead oxides offer a process with 50% and 61% exergy efficiency (at the reference condition for $H_2/CO=1$), respectively with methane production of less than 1%.

Acknowledgement

Authors of this work gratefully acknowledge Australian Research Council (ARC) for the financial support through grant DP150102230. The first author of this work acknowledges "Australian Government Research Training Program Scholarship" for the financial supports.

Nomenclature

C_p	Heat capacity, kJ/kg
H	Enthalpy, kJ
M	Enthalpy or Gibbs free energy, kJ (See eq. (5))
T	Temperature, °C or K
y	Mole fraction of component
Superscripts and Subscripts	
i	component
f	formation
Greek letters	
Δ	difference
χ	Temperature difference between reactors, °C or K
γ	Production extent (mole fraction of components)
Abbreviations	
g	Gas
LCLC	Liquid chemical looping combustion
LCLG	Liquid chemical looping gasification
LOC	Liquid oxygen carrier
Me	Metal oxide
Oxid	Oxidation
Prod	product
Reac	Reactant
Red	Reduction
Redox	Reduction-Oxidation
S	Solid

References

[1] Adanez J, Abad A, Garcia-Labiano F, Gayan P, Luis F. Progress in chemical-looping combustion and reforming technologies. Progress in Energy and Combustion Science. 2012;38:215-82.
[2] Kenarsari SD, Yang D, Jiang G, Zhang S, Wang J, Russell AG, et al. Review of recent advances in carbon dioxide separation and capture. Rsc Advances. 2013;3:22739-73.
[3] Lyngfelt A, Kronberger B, Adanez J, Morin J, Hurst P. The GRACE project. Development of oxygen carrier particles for chemical-looping combustion. Design and operation of a 10KW chemical-looping combustor: na; 2004.
[4] Leion H, Lyngfelt A, Johansson M, Jerndal E, Mattisson T. The use of ilmenite as an oxygen carrier in chemical-looping combustion. Chemical Engineering Research and Design. 2008;86:1017-26.
[5] Linderholm C, Mattisson T, Lyngfelt A. Long-term integrity testing of spray-dried particles in a 10-kW chemical-looping combustor using natural gas as fuel. Fuel. 2009;88:2083-96.
[6] Johansson M, Mattisson T, Lyngfelt A. Use of NiO/NiAl2O4 particles in a 10 kW chemical-looping combustor. Industrial & Engineering Chemistry Research. 2006;45:5911-9.
[7] Forero C, Gayán P, García-Labiano F, De Diego L, Abad A, Adánez J. High temperature behaviour of a CuO/γAl 2 O 3 oxygen carrier for chemical-looping combustion. International Journal of Greenhouse Gas Control. 2011;5:659-67.
[8] M. Jafarian MA, G. Nathan. High temperature chemical looping combustion using molten iron oxide as the oxygen carrier. Industrial & Engineering Chemistry Process Design and Development. 2016;in press:1-14.
[9] LaMont DC, Seaba J, Latimer EG, Platon A. Liquid-phase chemical looping energy generator. Google Patents; 2011.
[10] McGlashan N. Chemical-looping combustion—a thermodynamic study. Proceedings of the Institution of Mechanical Engineers, Part C: Journal of Mechanical Engineering Science. 2008;222:1005-19.
[11] McGlashan NR, Childs PR, Heyes AL, Marquis AJ. Producing hydrogen and power using chemical looping combustion and water-gas shift. Journal of Engineering for Gas Turbines and Power. 2010;132:031401.
[12] McGlashan NR, Childs PR, Heyes AL. Chemical looping combustion using the direct combustion of liquid metal in a gas turbine based cycle. Journal of Engineering for Gas Turbines and Power. 2011;133:031701.
[13] Cho P, Mattisson T, Lyngfelt A. Comparison of iron-, nickel-, copper-and manganese-based oxygen carriers for chemical-looping combustion. Fuel. 2004;83:1215-25.
[14] Wang K, Yu Q, Qin Q. The thermodynamic method for selecting oxygen carriers used for chemical looping air separation. Journal of thermal analysis and calorimetry. 2013;112:747-53.

[15] Jerndal E, Mattisson T, Lyngfelt A. Thermal Analysis of Chemical-Looping Combustion. Chemical Engineering Research and Design. 2006;84:795-806.

[16] Lyngfelt A, Leckner B, Mattisson T. A fluidized-bed combustion process with inherent CO_2 separation; application of chemical-looping combustion. Chemical Engineering Science. 2001;56:3101-13.

[17] Enghag P. Encyclopedia of the elements: technical data-history-processing-applications: John Wiley & Sons; 2008.

[18] Patnaik P. Handbook of inorganic chemicals: McGraw-Hill New York; 2003.

[19] Feher F, Brauer G. Handbook of Preparative Inorganic Chemistry. Academic Press, New York. 1963:341.

[20] Smith WF, Hashemi J. Foundations of materials science and engineering: McGraw-Hill; 2011.

[21] File END, Part B, Version V. National Nuclear Data Center. Brookhaven National Laboratory. 1990.

[22] Chadwick SS. Ullmann's Encyclopedia of Industrial Chemistry. Reference Services Review. 1988;16:31-4.

[23] Morrow H. Cadmium and cadmium alloys. Kirk-Othmer Encyclopedia of Chemical Technology. 2001.

[24] Price GD. Mineral Physics: Treatise on Geophysics: Elsevier; 2010.

[25] Hay J, Pharr G. ASM Handbook: Mechanical testing and evaluation. ASM International. 2000;8:232.

[26] Cotton FA, Wilkinson G, Murillo CA, Bochmann M, Grimes R. Advanced inorganic chemistry: Wiley New York; 1999.

[27] Barin I. Thermochemical Data of Pure Substances, Thermochemical Data of Pure Substances: Wiley-VCH; 1997.

[28] Yun Y, Chung SW, Yoo YD. Syngas quality in gasification of high moisture municipal solid wastes. Prepr Pap-Am Chem Soc, Div Fuel Chem. 2003;48:823.